Noninvasive Monitoring of Tissue Temperature Changes Induced by Focused Ultrasound Exposure using Sparse Expression of Ultrasonic Radio Frequency Echo Signals

Abstract

Background: Noninvasive therapies such as focused ultrasound were developed to be used for cancer therapies, vessel bleeding, and drug delivery. The main purpose of focused ultrasound therapy is to affect regions of interest (ROI) of tissues without any injuries to surrounding tissues. In this regard, an appropriate monitoring method is required to control the treatment. **Methods:** This study is aimed to develop a noninvasive monitoring technique of focused ultrasound (US) treatment using sparse representation of US radio frequency (RF) echo signals. To this end, reasonable results in temperature change estimation in the tissue under focused US radiation were obtained by utilizing algorithms related to sparse optimization as orthogonal matching pursuit (OMP) and accompanying Shannon's entropy. Consequently, ex vivo tissue experimental tests yielded two datasets, including low-intensity focused US (LIFU) and high-intensity focused US (HIFU) data. The proposed processing method analyzed the ultrasonic RF echo signal and expressed it as a sparse signal and calculated the entropy of each frame. **Results:** The results indicated that the suggested approach could noninvasively estimate temperature changes between 37°C and 47°C during LIFU therapy. In addition, it represented temperature changes during HIFU ablation at various powers, ranging from 10 to 130 W. The normalized mean square error of the proposed method is 0.28, approximately 2.15 on previous related methods. **Conclusion:** These results demonstrated that this novel proposed approach, including the combination of sparsity and Shanoon's entropy, is more feasible and effective in temperature change estimation than its predecessors.

Keywords: *Entropy, high-intensity focused ultrasound, low-intensity focused ultrasound, sparse representation, thermometry*

Kiarash Behnam Malekzadeh[1], Hamid Behnam[1], Jahangir (Jahan) Tavakkoli[2,3]

[1]*Department of Biomedical Engineering, School of Electrical Engineering, Iran University of Science and Technology, Tehran, Iran,* [2]*Department of Physics, Toronto Metropolitan University,* [3]*Institute for Biomedical Engineering, Science and Technology (iBEST), Keenan Research Centre for Biomedical Sciences, St. Michael's Hospital, Toronto, ON, Canada*

Introduction

Open surgeries are the most common treatment for tumors, specifically solid tumors, but it is invasive, expensive, and has side effects. As a result, several noninvasive methods have been perused to improve therapeutic efficacy and patient comfort. One major noninvasive technique currently utilized is radiation therapy which radiates ionizing X-ray beams to destroy cancer cells. However, X-ray radiation can cause potential side effects, necessitating determining the optimal dose and monitoring throughout treatments.[1]

Another promising noninvasive technique for treating cancer cells is high-intensity focused ultrasound (HIFU). In this treatment, ultrasound (US) waves are focused on the regions of interest (ROI) to heat and ablate abnormal tissue and cells. Compared to radiation therapy, it is cost efficient, nonionizing, and harmless for surrounding tissues. Furthermore, HIFU therapy can be performed repeatedly due to its minimal side effects. However, it is unsuitable for tumors in organs such as the lungs and bowel because of the high attenuation of US waves in the air and bone. In spite of these limitations, HIFU is an intriguing method that can treat cancer tumors noninvasively and without severe side effects. Thus, HIFU therapy has been applied to numerous types of cancerous tumors in organs such as the liver, kidney, prostate, breast, and uterine.[1]

Address for correspondence:
Dr. Hamid Behnam,
Department of Electrical Engineering, Iran University of Science and Technology, Tehran, Iran.
E-mail: behnam@iust.ac.ir

How to cite this article: Malekzadeh KB, Behnam H, Tavakkoli J. Noninvasive monitoring of tissue temperature changes induced by focused ultrasound exposure using sparse expression of ultrasonic radio frequency echo signals. J Med Sign Sens 2024;14:8.

HIFU is a noninvasive technique that induces selective thermal and mechanical effects in a ROI.[2] In this method, the thermal effect depends on the focal spot's temperature increase due to the absorption of US. This increase can depend on the intensity and duration of the treatment, resulting in various stages of tissue or cell destruction, ranging from reversible heat-induced changes (43°C–45°C) to coagulation necrosis at temperatures above 50°C. Mechanical effects induced by HIFU involve nonthermal tissue destruction and are associated with high-intensity acoustic pulses, resulting in cavitation, microstreaming, and radiation force, leading to the disruption of the vascular structure, connective tissue, and cellular damage.[3] HIFU requires a suitable imaging technique to envisage the target and monitor the treatment process. While imaging guidance can potentially increase clinical use and broaden HIFU's applications, which imaging platform should be used remains debatable.[4]

Currently, two types of imaging systems are integrated with HIFU: magnetic resonance imaging-guided (MRI) and US-guided procedures. While substantial device-specific variations may exist, the underlying process is generally consistent. Both methods have proponents and opponents. The US-guided procedures are inexpensive and convenient and may be performed in real time, where MR-HIFU can provide high-quality resolution images and better thermometry data.[5] MRI systems are typically used to confirm the ROI and measure the corresponding temperature clinically. MRI is a suitable imaging modality that can provide volumetric images. Nevertheless, it has the following limitations: (1) setting up the system requires a large space and is quite costly, (2) it must be compatible with all other devices, including HIFU, and (3) MRI has a low temporal resolution. US imaging can also evaluate and differentiate the temperature rise by tracking the shifts in speckle patterns caused by changes in the speed of sound. Even though US images have cost effective, real-time imaging capability, and high temporal resolution, they are prone to excessive noise and artifacts that limit its adoption for clinical applications.[1]

US thermometry is a simple and portable method that may be more effective than other methods. The leading US thermometry methods for hyperthermia therapies, in which the tissue temperature does not transgress 45°C, are currently based on the signal changes in backscattered energy (CBE), the backscattered radio frequency (RF) echo shift due to a change in the speed of sound, and in amplitudes of the acoustic harmonics.[6] Among these techniques, the backscattered RF echo shift is currently the most established, and its viability in small animals has been demonstrated *in vivo*. Nevertheless, the echo-shift method is highly sensitive to tissue motion.[6]

The US thermometry method based on CBE of the acoustic harmonics is used to estimate the temperature in *ex vivo*

tissues. Moreover, the feasibility of using the CBE method to identify heated ROI generated by low-intensity focused US (LIFU) and to control the temperature in the heated region has been demonstrated.[6] Such control systems can be used for targeted drug delivery applications, where keeping the temperature between 41°C and 45°C for a few minutes is adequate to release the drugs.[6]

In addition, entropy imaging is a technique that can quantify the uncertainty of a random process and is usually utilized as a measure for probability distributions.[7] Shannon's entropy of RF time series signal possesses promising features which show that the change of the entropy parameter of the RF time series signal is proportional to temperature changes recorded by a calibrated thermocouple in the temperature range of 37°C–47°C by considering the uncertainty in given data that can be used, as a method, to measure temperature changes noninvasively and quantitatively in the deep region of tissue.[7] In entropy method (Behnia *et al.*[7]), they prepared time series of consecutive B-mode images. When all amplitude values in the time series are the same, the entropy is 0, and when every amplitude value is unique, it is 1.28. Spatiotemporal interpolation is carried out on the final results of their study by a cubic spline function.[7]

Compressive sensing (CS) and sparse representation have become more prevalent in signal and image processing applications, such as pattern recognition and machine vision. To the best of our knowledge, however, there has been limited research on CS for US signal and image reconstruction. The number of measurements in CS can be significantly less than the number of samples typically taken in the traditional sampling method known as the Nyquist rate.[8]

In general, signal reconstruction from CS measurements is performed through optimization algorithms. The signal is contaminated with various noises and artifacts in many medical and engineering applications. In addition to corrupting the original signal, noise and artifacts also impact the reconstructed signal. To this end, CS theory can be applied as a method for reducing noise if the sparse space of the signal is known.[9] This fact is attributable to two causes: signal and noise are relatively distinct in sparse space, and the number of measurements can only contain limited information about noise and artifacts. Multiple studies have demonstrated that CS can be used for two main purposes: (1) it can reduce the amount of data required, thereby increasing the speed of data acquisition and (2) it can be used in applications with data recording limitations.[8] *Ex vivo* porcine muscle tissue was used for all experiments and results in the current study.[7,9]

In mentioned methods, the CS method (Ghasemifard *et al.*[8,9]) was applied for HIFU lesion detection. In addition,

the entropy (Behnia *et al.*[7]) and the CBE (Shaswary *et al.*[6]) methods were applied for LIFU thermometry. Citing past articles, utilizing a combination of sparsity or CS and other related methods as the entropy could be feasible to improve the monitoring method of focused US because sparsity would reduce the amount of data and noise.

The analysis results demonstrated the novel proposed method's effectiveness for the noninvasive monitoring of tissue changes induced by both LIFU radiation and HIFU thermal lesion production.

Materials and Methods

Two types of data were used for the analysis in this study. The data were recorded in the Advanced Biomedical US Imaging and Therapy Laboratory in the Department of Physics at Toronto Metropolitan University (formerly Ryerson University), Toronto, Canada, and the Institute for Biomedical Engineering, Science, and Technology, Keenan Research Center for Biomedical Science, St. Michael's Hospital, Toronto, Ontario, Canada.

Dataset 1: Low-intensity focused ultrasound data

Ex vivo excised pork muscle tissue obtained from a local butchery was immersed in 0.9% saline solution at 5°C for 24 h. The tissue sample was placed in a holder, where the dimensions of the tissue sample were 5 cm × 8 cm × 3 cm (axial × lateral × height). The holder was subsequently placed in a water tank with a single-element focused therapeutic transducer (Imasonic SAS, Voray sur l'Ognon, France) operating in the LIFU range. A schematic diagram of the setup is shown in Figure 1 (reproduced from[6]).

The central frequency of the LIFU transducer was 1 MHz, its focal length was 100 mm, and its aperture diameter was 125 mm. The temperature of the tank's water was fixed and controlled at 37°C by a circulating water bath (Haake DC10, Thermo Electron Corp., Newington, NH, USA). The LIFU transducer was derived by a 175 mVpp input signal (corresponding to an acoustic output power of 4.5 W) for 1000 cycles at 1 MHz, with a duty cycle of 50%. The base temperature was 37°C, and the temperature in the focal zone reached 47°C after 6 min of exposure. The simulated intensity field of the therapeutic transducer produced by an acoustic scope and temperature response simulator (LATS) is shown in Figure 2.

Because of utilizing the same LIFU dataset, more details about data acquisition and equipment have been mentioned in references Behnia *et al.*[7] and Shaswary *et al.*[6]
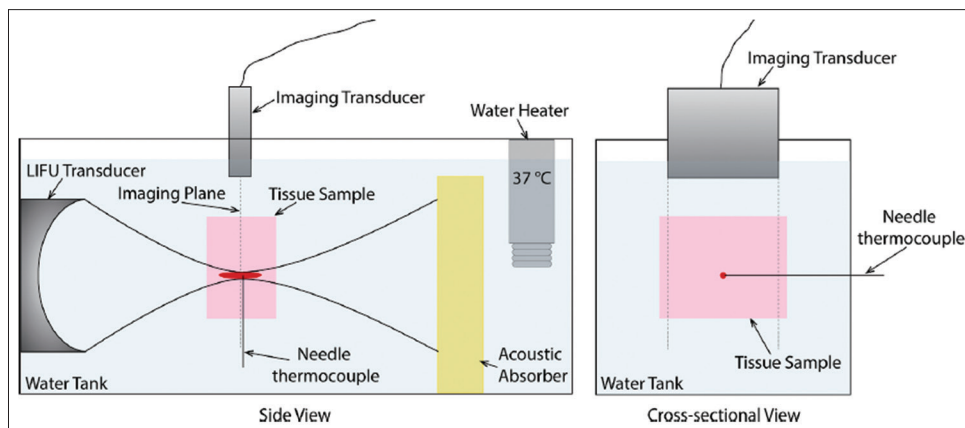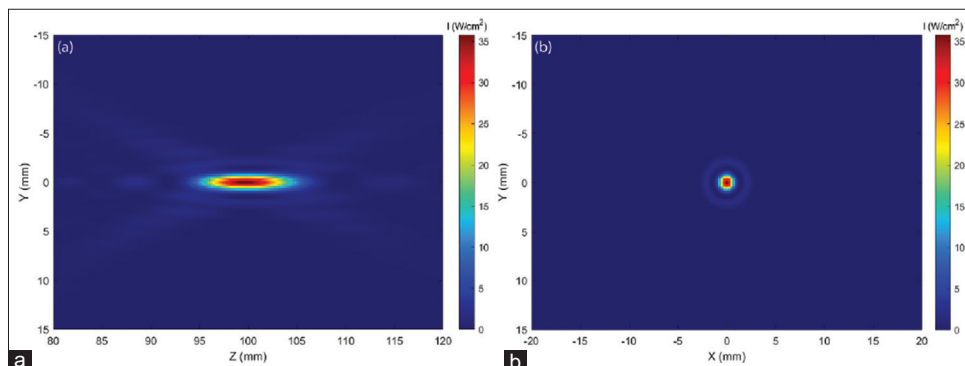

Figure 1: The experimental setup[6]

Figure 2: Simulated low-intensity focused ultrasound transducer intensity field in (a) side (b) cross-sectional views. The field was generated using a linear acoustic and temperature simulator[6]

In the first set of experiments, a thermocouple was placed at the focus of the therapeutic transducer, and the temperature of the tissue was recorded as it was exposed to LIFU. Due to thermocouple artifacts, no backscattered RF data were collected during these experiments. In the second set of experiments, the thermocouple was removed from the tissue before exposure to LIFU with the same exposure parameters as the first set. This was repeated five times for different tissue samples.[6]

Dataset 2: High-intensity focused ultrasound data

In this experiment, porcine muscle tissue was exposed to HIFU exposure *in vitro*. To this end, a piezo composite single-element spherically focused HIFU transducer (Model 6699A101, Imasonic SAS, Voray sur l'Ognon, France) with a frequency of 1 MHz and aperture diameter of 125 mm was used. It is the same transduc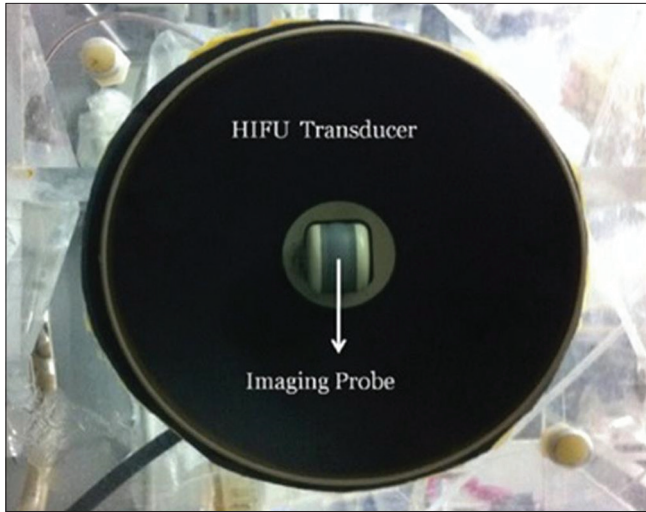er used in the LIFU study. They just increased its deriving input voltage and the acoustic power to run it in the HIFU mode. In addition, an US imaging system (Sonix RP scanner, Ultrasonix Inc., Richmond, BC, Canada) was utilized to record US images and RF echo signals data. The imaging probe and the HIFU transducer were assembled in a confocal arrangement [Figure 3]. The timing sequence of the HIFU exposure is shown in Figure 4. Because of utilizing the same HIFU dataset, more details about data acquisition and equipment have been mentioned in references Ghasemifard *et al*.[8,9] and Rangraz *et al*.[10]

Data acquisition and processing methodology

The data obtained in this study were processed using MATLAB software (MATLAB 2018b, The MathWorks Inc., California, USA). The RF US echo signals from the ROI were selected in the first step based on the considered data, one of which was the US images obtained during the LIFU treatment, and the other data were the US images obtained during the HIFU treatment. This space was defined by considering the images in the frames and the information above and subsequently subjected to the basic transformation, which included the Hilbert transform and absolute magnitude as follows Eq. 1:

$$y = abs\left(Hilbert\left(x\right)\right)$$

Figure 3: Confocal arrangement of the imaging probe and the high-intensity focused ultrasound transducer[8]
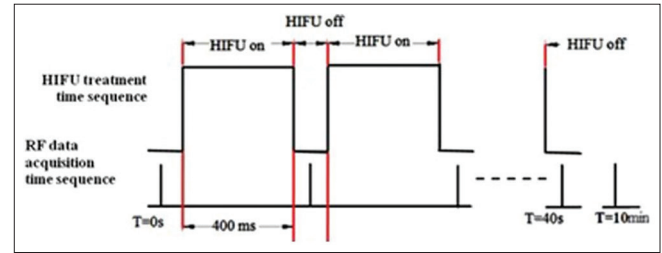

Figure 4: The timing sequence of high-intensity focused ultrasound exposure and radio frequency echo data acquisition[8]
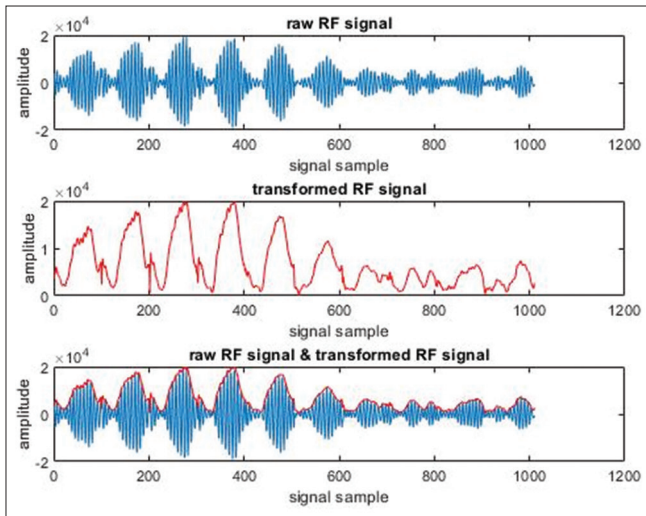

Figure 5: Illustration and comparison of the radio frequency signal of an arbitrary frame (frame 2) in the regions of interest before and after the initial transformation using low-intensity focused ultrasound data
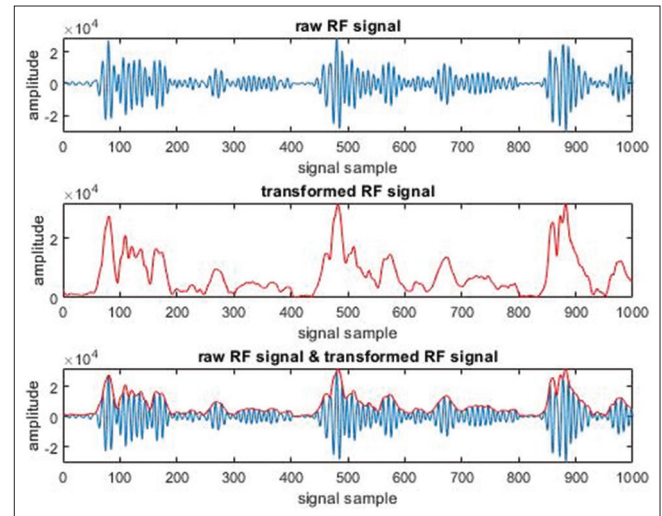

Figure 6: Illustration and comparison of the radio frequency signal of an arbitrary frame (frame 2) in the regions of interest before and after the initial transformation using high-intensity focused ultrasound data

Example images of RF signal changes before and after initial conversion are shown in Figures 5 and 6.

In the second step, the obtained signal was fed into the sparse optimization algorithm to obtain atoms with the aid of a well-designed dictionary that can be used to reconstruct the signal and create the reconstructed sparse signal. In this study, the greedy orthogonal matching pursuit (OMP) algorithm (Retrieved from https://sparse-plex.readthedocs.io/en/latest/book/complexity/omp.html) was used, which, according to previous research, has a low computational speed but an excellent approximation of signal reconstruction.[11] The pseudo-code of the OMP is shown in Figure 7.

$$x, r, \Lambda = \text{OMP}(\Phi, y);$$
$$x^0 \leftarrow 0;$$
$$r^0 \leftarrow y; \qquad\qquad\qquad // \ r = y - \Phi x$$
$$\Lambda^0 = \varnothing; \qquad\qquad // \ \text{Index set of chosen atoms}$$
$$k \leftarrow 0; \qquad\qquad\qquad // \ \text{Iteration counter}$$
repeat
$$\quad h^{k+1} \leftarrow \Phi^T r^k; \qquad\qquad // \ \text{Match}$$
$$\quad \lambda^{k+1} = \underset{j \notin \Lambda^k}{\arg\max} |h_j^{k+1}|; \qquad // \ \text{Identify}$$
$$\quad \Lambda^{k+1} \leftarrow \Lambda^k \cup \{\lambda^{k+1}\}; \qquad // \ \text{Update support}$$
$$\quad x^{k+1} \leftarrow 0;$$
$$\quad x_{\Lambda^{k+1}}^{k+1} \leftarrow \Phi_{\Lambda^{k+1}}^\dagger y; \quad // \ \text{Update representation LS}$$
$$\quad y^{k+1} = \Phi x^{k+1}; \qquad\qquad // \ \text{Update approximation}$$
$$\quad r^{k+1} \leftarrow y - y^{k+1}; \qquad\qquad // \ \text{Update residual}$$
$$\quad k \leftarrow k + 1; \qquad // \ \text{Update iteration counter}$$
until *halting criteria is satisfied*;
$$x \leftarrow x^k; \ \Lambda \leftarrow \Lambda^k; \ r \leftarrow r^k;$$

Figure 7: Different stages of the orthogonal matching pursuit algorithm

For accurate signal reconstruction, we arrived on wavelet family bases, including Daubechies wavelet (db), Symlet (sym), and discrete Meyer (dmey), where db4, sym2, sym4, and dmey constitute this dictionary, respectively. Figure 8 depicts the wavelet images and scaling of the aforementioned wavelet packets.

According to the specified algorithm and dictionary that we used, the greedy OMP algorithm yields one atom each time it is executed. With 100 algorithm iterations (by evaluating different iterations between 50 and 500 these 100 iterations have been chosen) and 100 nonzero coefficients, we were able to reconstruct the signal and obtain a sparse signal of the desired quality after extensive investigation.

It should be noted that the dictionary is designed according to experience, test, and based on Gifani's dictionary (Gifani *et al*.[11]). Further, the designed dictionary is a rectangular matrix with dimensions ratio of 4 (the number of columns is four times the rows), for example, for a signal with a length of 10,000 samples, the dictionary matrix has 10,000 rows, 40,000 columns, and does not follow the properties of a square matrix. For this reason, the OMP algorithm has been used. Furthermore, we have 40,000 atoms.

Afterward, we entered the entropy portion of the processing. This implementation of the sparse algorithm will reduce the noise in the signal, and it is predicted that the signal will behave more favorably than demonstrated by the previous research. Figures 9 and 10 depict an example of the signal image generated by the OMP algorithm with 100 iterations.
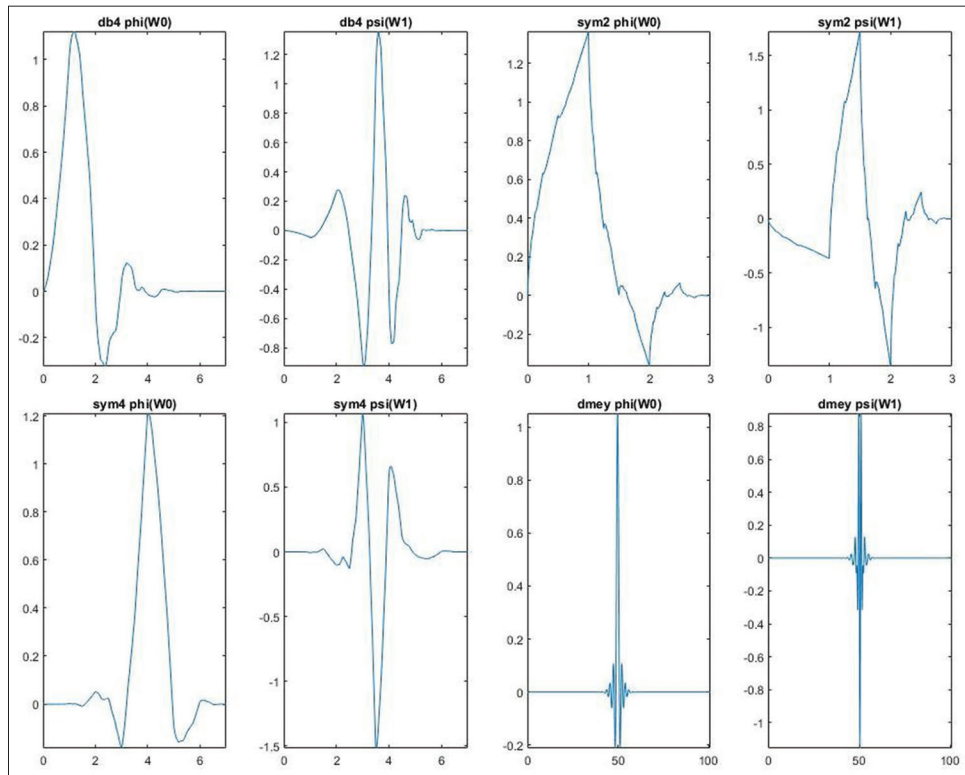

Figure 8: Wavelet packets utilized in the dictionary design
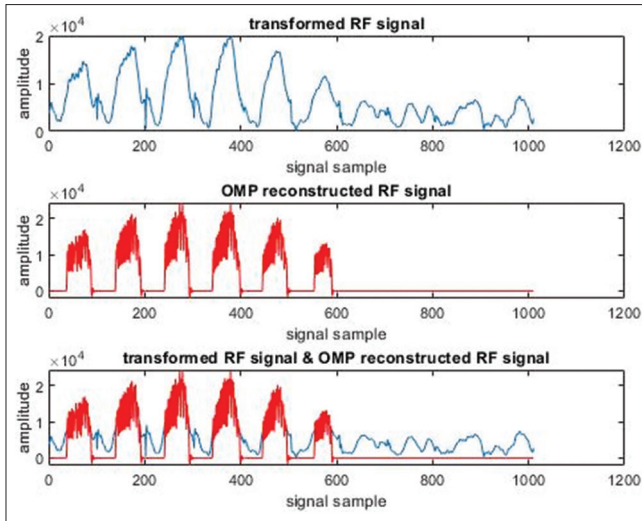
Figure 9: Illustration and comparison of the radio frequency signal of an arbitrary frame (frame 2) before and after the sparse algorithm in low-intensity focused ultrasound data
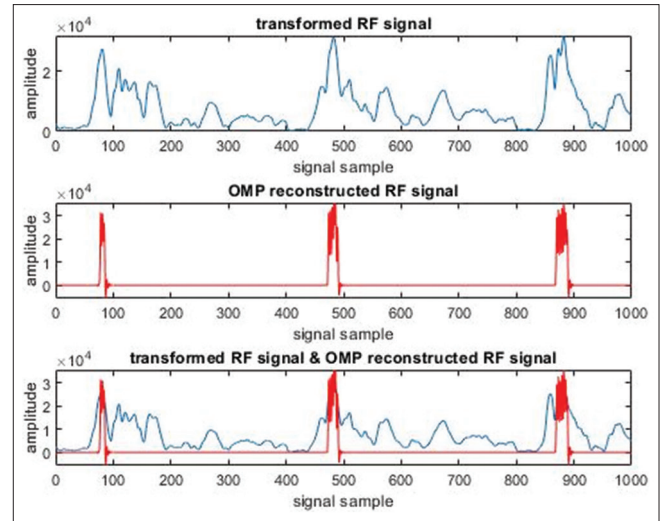

Figure 10: Illustration and comparison of the radio frequency signal of an arbitrary frame (frame 2) before and after the sparse algorithm in high-intensity focused ultrasound data
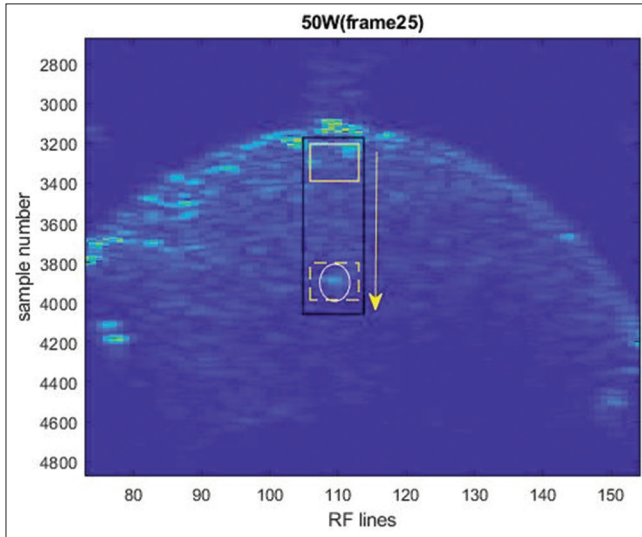

Figure 11: Schematic of the hypothetical window for the thermal distribution in an arbitrary frame of high-intensity focused ultrasound data

The third and final step of the proposed method was the application of the entropy criterion, wherein Shannon's entropy (Retrieved from https://en.wikipedia.org/wiki/Entropy_(information_theory)) was used as follows after multiple types of entropies had been evaluated Eq. 2:

$$H(x) = -\sum_{x=1}^{N} p(x) \log p(x) = \mathbb{E}[-\log p(x)]$$

The method was applied to measure the signal obtained from the region of interest in each image frame after conversion and reconstruction by the stated algorithm by the Shannon entropy criterion. Then, the entropy values obtained from each signal were arranged in the order of the frames, where a signal was then displayed in terms of entropy changes in consecutive frames. This method

was evaluated using LIFU data, where the results of the proposed method are provided in the results section.

In the continuation of the study, an attempt was made to determine the temperature distribution in a hypothetical 1 cm × 1 cm window within the ROI of the tissue. This method was developed by calculating entropy and is more accurate in the specified region. Notably, after analyzing this method on both datasets, it was determined that it is more precise and valuable for focal US data, as it can help detect the thermal lesion and reveal temperature changes.

As per Figure 11, in the black rectangle representing the investigated region, we extracted a portion of the space using a square window (Yellow Square) and processed its signal using the proposed method. Then, based on the direction of the arrow, we proceeded to the subsequent squares in that region and implemented the method to examine its output in successive frames. In addition, the region of lesion formation denoted with a white circle in the figure should be identifiable in the final image of this thermal distribution.

Results

This section presents the results of the desired processing method. First, the results of this method are compared to the LIFU data and then to the HIFU data.

In the first six frames of data related to LIFU, the application of LIFU causes an increase in temperature. The subsequent phase is tissue cooling. By processing RF US signals in different frames in the region of interest using the previously mentioned steps of the proposed method, which included the Hilbert transform, sparse reconstruction algorithm with a newly designed dictionary, and Shannon entropy. Figure 12 depicts an example of the processing
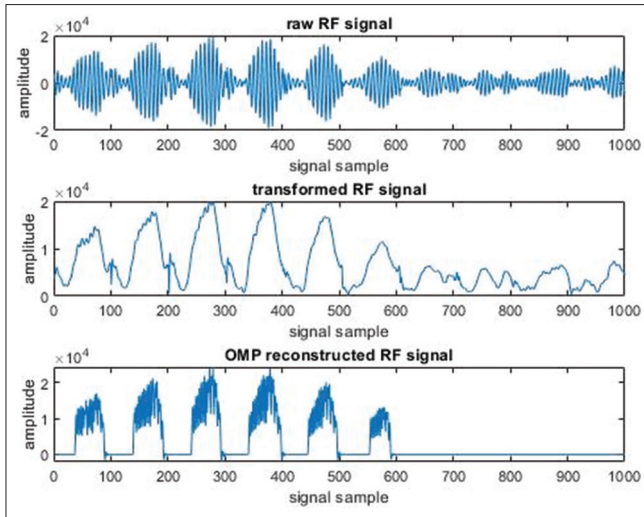
Figure 12: The first two stages of the proposed method based on the arbitrary frame's (frame 2) signal in low-intensity focused ultrasound data
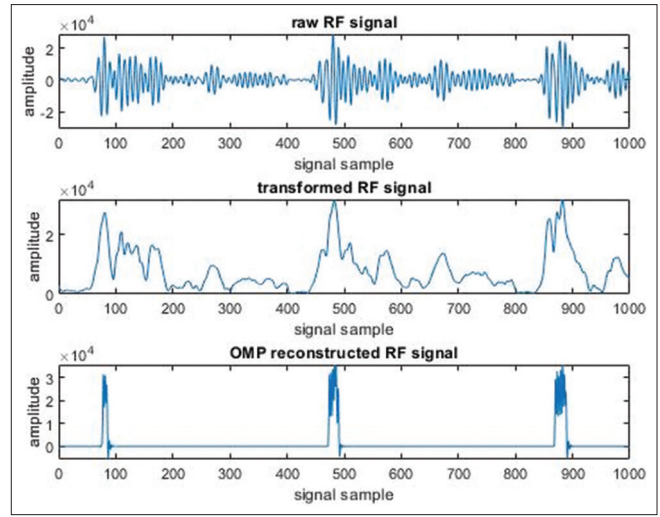

Figure 13: The first two stages of the proposed method based on the arbitrary frame's (frame 2) signal in low-intensity focused ultrasound data
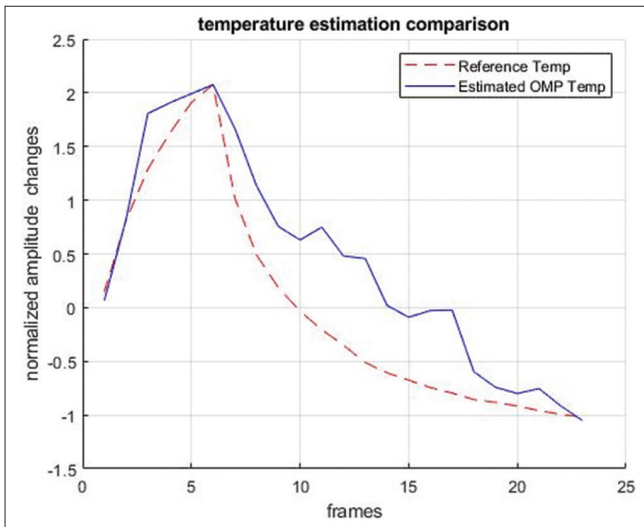

Figure 14: The result of the proposed method for temperature change estimation of low-intensity focused ultrasound data
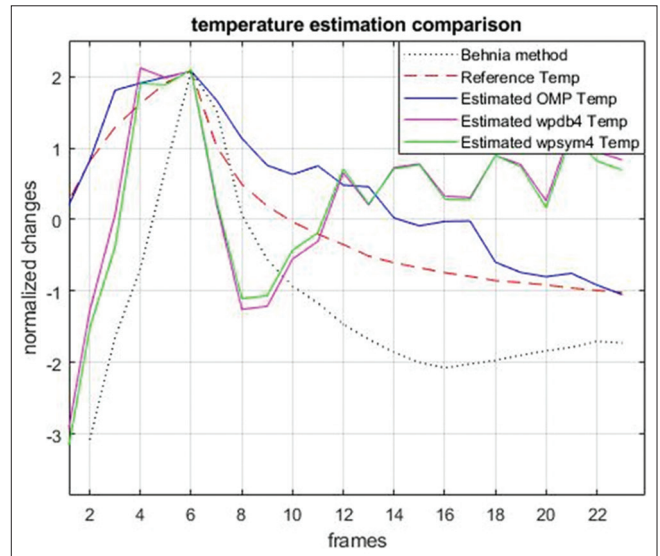

Figure 15: Comparison of the proposed method's results with those of previously suggested methods
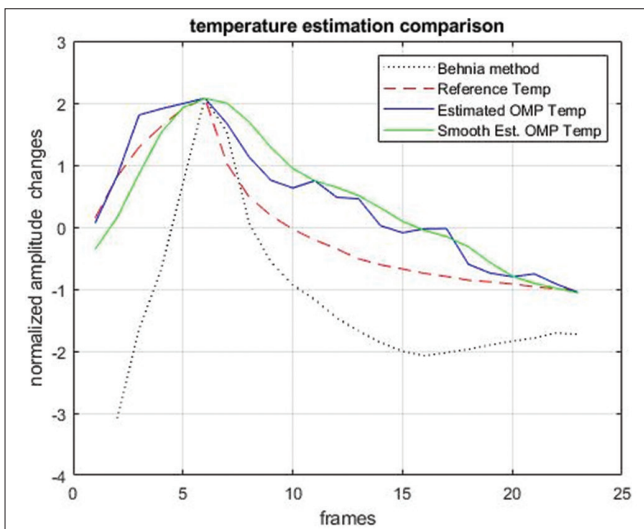

Figure 16: Comparison of the proposed method's results with those of a previous related study

steps performed on the RF signal, whereas Figure 13 illustrates an RF line in greater detail. Subsequently, the final result for all frames is provided in Figure 14.

Following the steps outlined above, Shannon's entropy was extracted from the signal of each frame, and the entropy values of the frames were placed next to one another to demonstrate the temperature change estimation.

In advance, we have tested wavelet transforms instead of an experimentally designed dictionary and the OMP algorithm. The results were unacceptable, so the proposed method changed to the OMP algorithm. The comparison of the wavelet transforms results and the proposed method is shown below in Figure 15.

In this regard, the normalized mean square error of Figure 15 methods is shown in Table 1.

Method's name	Normalized mean square error
Behnia *et al.*[7]	2.1526
Daubechies4 wavelet packet transform	2.2137
Symlet4 wavelet packet transform	2.2596
Proposed OMP and dict	0.2829

OMP – Orthogonal matching pursuit
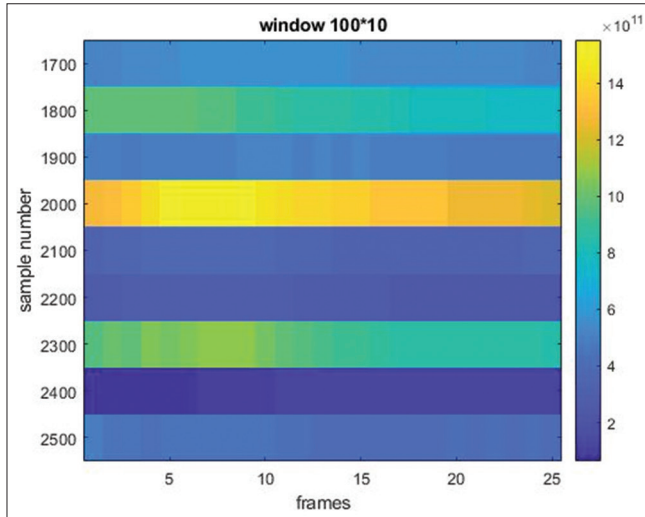
Figure 17: Tissue thermal distribution during low-intensity focused ultrasound radiation as measured by 100 sample windows and 10 radio frequency lines

After comparing the result of estimating changes with the thermocouple's measured temperature, the proposed method was compared to previous results (Behnia *et al.*[7]). Although the LIFU dataset and Shannon entropy are the same in all methods, they are different at all. Obviously, the normalized mean square error showed the difference between these methods, and the novelty of combining sparsity and entropy improved the temperature estimation. In addition, a Gaussian filter was used to smooth the curve. The results are depicted in Figure 16. Notably, the filter utilized by the MATLAB software was a Gaussian-weighted moving average.

As depicted in Figure 16 and Table 1, the performance of the proposed method for estimating the temperature changes of the target tissue is superior to that of the previous methods, with the manner of changes being much closer to those of the thermocouple that is considered the reference temperature. Using the proposed method, we attempted to depict these modifications as a heat distribution map, the result of which is shown in Figure 17.

As evident in Figure 17, at a depth of approximately 47 mm (samples points 2000–2099), the focal point of LIFU radiation, the same temperature changes are observed as in Figure 14.

The proposed method was then applied to the second dataset (HIFU) to compare its efficiency at different powers. This dataset contains the US produced at 10 W (217 W/cm^2), 30 W (650 W/cm^2), 50 W (1084 W/cm^2), 70 W (1517 W/cm^2), 90 W (1951 W/cm^2), and 110 W (2384 W/cm^2). As expected, temperature changes and lesions were observed, as shown in Figure 18.

Compared to the changes in the frames, the variations in temperature and the location of the lesion are evident in Figure 18. Moreover, according to the cited articles, the displacement observed in the image, particularly at high powers, can be attributed to the effect of changes in the speed of sound due to the tissue temperature changes. The speed of sound is temperature dependent, and the time delay is proportional to the speed of sound.[12] Due to the lack of a common scale in previous images, it is difficult to comprehend the effect of HIFU exposure on the formation of a lesion. Figure 19 displays images with a common scale to address this issue.

Discussion

After reviewing previous studies and numerous tests, the current study aimed to develop a novel method based on the two experiments, for which data were available, LIFU and HIFU. To this end, the sparse expression was utilized to reduce the computation and memory requirements for noninvasive real-time monitoring of focused ultrasound therapy. The OMP algorithm and Shannon entropy were successfully applied to RF US echo signals, yielding the expected results.

Further, Behnia *et al.*'s[7] article is about using Shannon entropy on frames, but the proposed method is a combination of sparse representation and entropy on signals. Although the LIFU dataset and Shannon entropy are the same in both methods, they are different at all. Obviously, the normalized mean square error showed the difference between these methods and the novelty of combining sparsity and entropy improved the temperature estimation. In addition to all the method's benefits, several potential areas can be investigated in future; some of the recommended ones include:

- Examining the dictionary learning algorithm instead of the designed dictionary
- Investigating other sparsity algorithms, such as Bayesian compressive sensing (BCS), as an alternative to the OMP algorithm
- Evaluating the proposed method on other different data with various experimental conditions
- Evaluating the proposed method on the tissue of a living organism *(in vivo)* and documenting its challenges.
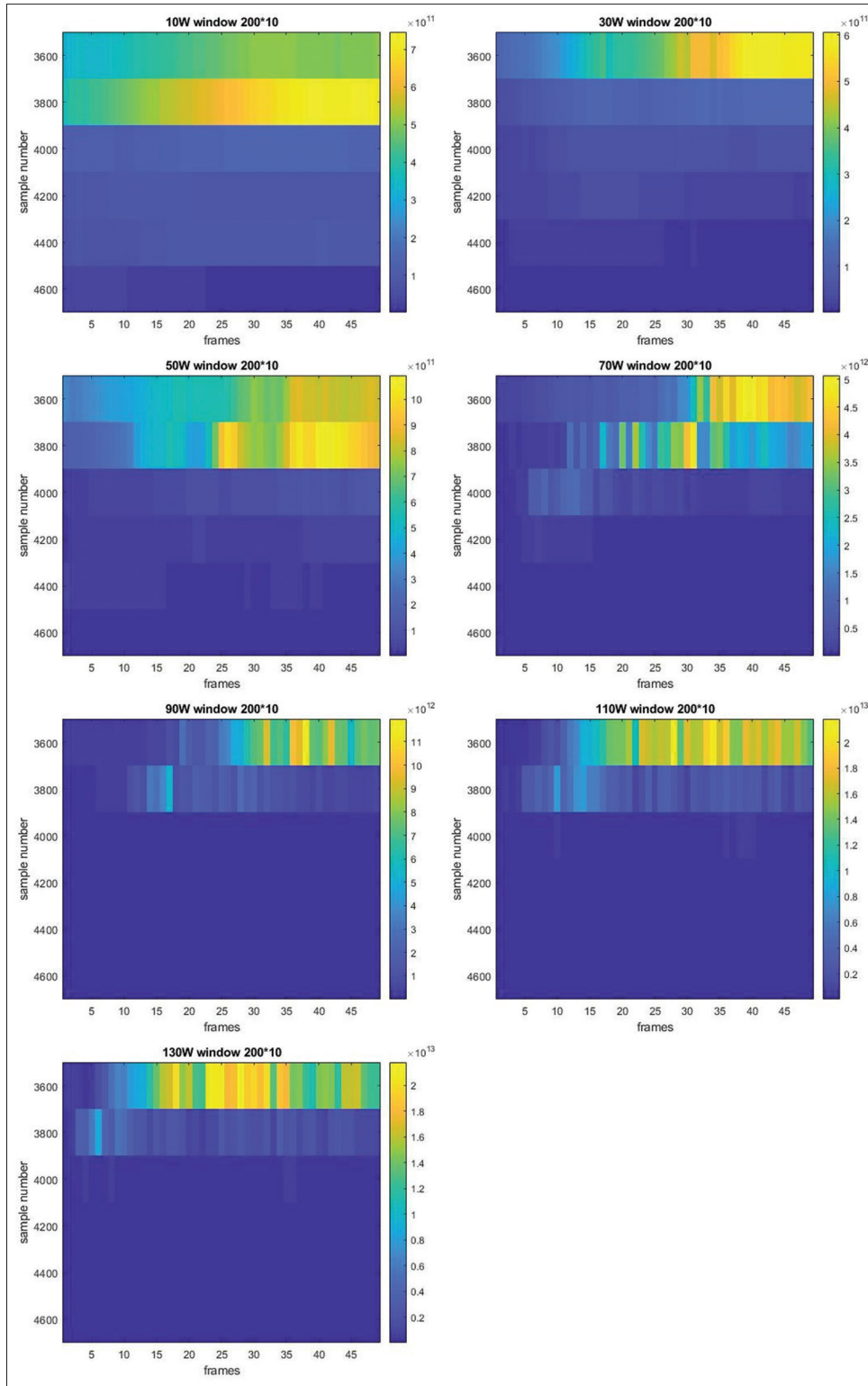
Figure 18: Tissue thermal distribution during high-intensity focused ultrasound radiation at different powers using windows of 200 samples and 10 radio frequency lines

Conclusion

This study attempted to demonstrate superior noninvasive monitoring of the tissue under focused ultrasound radiation through the sparse representation of the RF echo US signal, which was performed by reconstructing the signal via the OMP algorithm using a designed dictionary and a specified number of iterations. Temperature changes comparable to the reference temperature changes were estimated in the LIFU data, and the location of the lesion and tissue
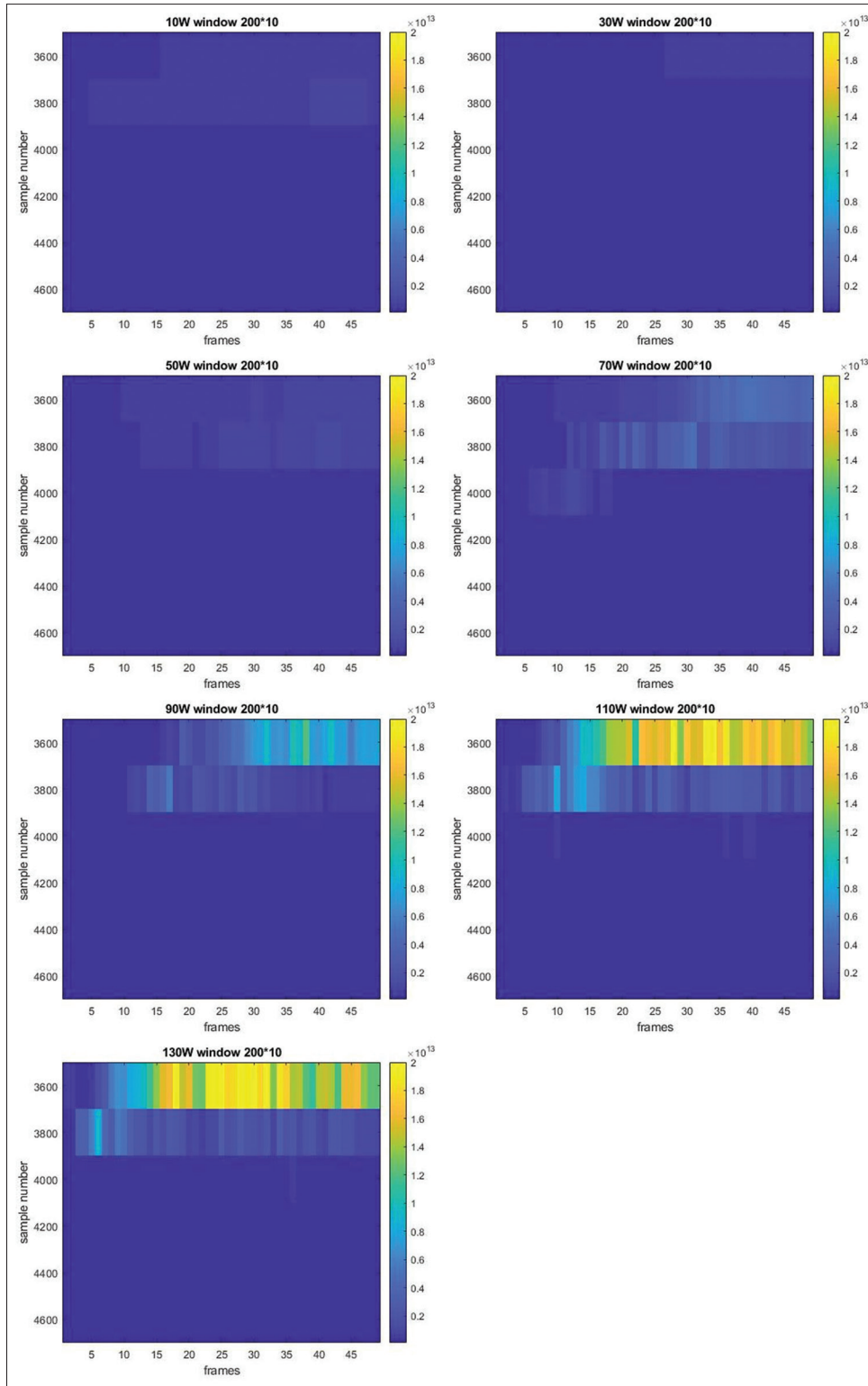
Figure 19: Tissue thermal distribution during high-intensity focused ultrasound radiation at different powers on a common scale by windows of 200 samples and 10 radio frequency lines

temperature changes at the ROI were estimated in the HIFU data. The results demonstrate the viability of the proposed noninvasive monitoring method for focused ultrasound in both LIFU and HIFU regimes.

Utilizing the primary transformation in conjunction with Shannon entropy was a novel technique that accompanied the OMP algorithm due to the similarities between the proposed method and previous articles. This innovation

was made more inclusive by the design of a new dictionary and its sparse representation. Furthermore, a novel concept made it possible to find a suitable and unique answer in a wide range of focused ultrasound power for which data was available using a designed dictionary and a specified number of algorithm iterations.

Financial support and sponsorship

None.

Conflicts of interest

There are no conflicts of interest.

References

1. Kim J, Choi WS, Park E, Kang Y, Lee KW, Kim HS, *et al*. Real-Time Photoacoustic Thermometry Combined With Clinical Ultrasound Imaging and High-Intensity Focused Ultrasound. IEEE Transactions on Biomedical Engineering 2019;66:3330-8. https://doi.org/10.1109/tbme.2019.2904087.

2. Alhamami M, Kolios MC, Tavakkoli J. Photoacoustic detection and optical spectroscopy of high-intensity focused ultrasound-induced thermal lesions in biologic tissue. Medical Physics 2014;41:053502. https://doi.org/10.1118/1.4871621.

3. Daoudi K, Hoogenboom M, Brok MH, Eikelenboom D, Adema GJ, Fütterer JJ, *et al*. In vivo photoacoustics and high frequency ultrasound imaging of mechanical high intensity focused ultrasound (HIFU) ablation. Biomedical Optics Express 2017;8:2235. https://doi.org/10.1364/boe.8.002235.

4. Cui H, Yang X. Real-time monitoring of high-intensity focused ultrasound ablations with photoacoustic technique: An in vitro study. Medical Physics 2011;38:5345-50. https://doi.org/10.1118/1.3638126.

5. Lozinski T, Filipowska J, Pyka M, Baczkowska M, Ciebiera M. Magnetic resonance-guided high-intensity ultrasound (MR-HIFU) in the treatment of symptomatic uterine fibroids — five-year experience. Ginekologia Polska 2021;93:185-94. https://doi.org/10.5603/gp.a2021.0098.

6. Shaswary E, Assi H, Yang C, Kumaradas JC, Kolios MC, Peyman G, *et al*. Noninvasive calibrated tissue temperature estimation using backscattered energy of acoustic harmonics. Ultrasonics 2021;114:106406. https://doi.org/10.1016/j.ultras.2021.106406.

7. Behnia A, Behnam H, Shaswary E, Tavakkoli J. Thermometry using entropy imaging of ultrasound radio frequency signal time series. Proceedings of the Institution of Mechanical Engineers, Part H: Journal of Engineering in Medicine 2022;236:1502-12. https://doi.org/10.1177/09544119221122645.

8. Ghasemifard H, Behnam H, Tavakkoli J. Toward high-intensity focused ultrasound lesion quantification using compressive sensing theory. Proceedings of the Institution of Mechanical Engineers, Part H: Journal of Engineering in Medicine 2017;231:1152-64. https://doi.org/10.1177/0954411917735557.

9. Ghasemifard H, Behnam H, Tavakkoli J. High-intensity focused ultrasound lesion detection using adaptive compressive sensing based on empirical mode decomposition. Journal of Medical Signals and Sensors 2019;9:24-32. https://doi.org/10.4103/jmss.jmss_17_18.

10. Rangraz P, Behnam H, Sobhebidari P, Tavakkoli J. Real-time monitoring of high-intensity focused ultrasound thermal therapy using the manifold learning method. Ultrasound in Medicine and Biology 2014;40:2841-50. https://doi.org/10.1016/j.ultrasmedbio.2014.07.021.

11. Gifani P, Behnam H, Haddadi F, Sani ZA, Shojaeifard M. Temporal super resolution enhancement of echocardiographic images based on sparse representation. IEEE Transactions on Ultrasonics Ferroelectrics and Frequency Control 2016;63:6-19. https://doi.org/10.1109/tuffc.2015.2493881.

12. Amiri H, Makkiabadi B. A Review of Ultrasound Thermometry Techniques. Frontiers in Biomedical Technologies 2020;7:82-91. https://doi.org/10.18502/fbt.v7i2.3852.